Coronary CT angiography in calcified coronary plaques: Comparison of diagnostic accuracy between bifurcation angle measurement and coronary lumen assessment for diagnosing significant coronary stenosis

Zhonghua Sun PhD[1], Lei Xu MD[2], Zhanming Fan MD[2]

1. Department of Medical Radiation Sciences, Curtin University, Perth, Western Australia, 6845, Australia
2. Department of Radiology, Beijing Anzhen Hospital, Capital Medical University, Beijing, 100029, China

Corresponding authors:

Prof Lei Xu, Department of Radiology, Beijing Anzhen Hospital, Capital Medical University, No. 2, Anzhen Road, Chaoyang District, 100029, Beijing, China

Tel: +86-10-64456071

Fax: +86-10-64456962

Email: leixu2001@hotmail.com

Prof Zhanming Fan, Department of Radiology, Beijing Anzhen Hospital, Capital Medical University, No. 2, Anzhen Road, Chaoyang District, 100029, Beijing, China

Tel: +86-10-64456310

Fax: +86-10-64456962

Email: fanzm120@126.com

Abstract

Background: To investigate the diagnostic value of coronary CT angiography (CCTA) by bifurcation angle measurement in the assessment of calcified plaques compared to the conventional coronary lumen analysis.

Methods: Fifty-three patients with calcified plaques identified on CCTA in the left coronary artery were included in the study. Minimal lumen diameter (MLD) and bifurcation angle between the left anterior descending (LAD) and left circumflex (LCx) were measured and compared between CCTA and invasive coronary angiography (ICA), while the areas under the curve (AUCs) by receiver-operating characteristic curve analysis (ROC) were compared between CCTA and ICA with regard to the diagnostic value of using bifurcation angle as a criterion.

Results: On a per-vessel assessment, the sensitivity, specificity, positive predictive value (PPV) and negative predictive value (NPV) and 95% confidence interval (CI) with use of bifurcation angle for determining coronary stenosis were 100% (86%, 100%), 79% (59%, 92%), 81% (62%, 92%), and 100% (85%, 100%) for CCTA, 100% (86%, 100%), 82% (63%, 94%), 83% (65%, 94%), and 100% (85%, 100%) for ICA, respectively. While the sensitivity and NPV remained unchanged, the specificity and PPV of CCTA by MLD were 33% (21%, 47%) and 43% (31%, 56%). The AUCs by ROC curve analysis for CCTA and ICA bifurcation angle measurements demonstrated no significant difference ($p>0.05$, 0.79 vs 0.86, and 0.70 vs 0.68 at the LAD and LCx assessment, respectively).

Conclusion: Coronary CT angiography by bifurcation angle measurement shows significant improvement in the diagnosis of calcified plaques with diagnostic value comparable to invasive coronary angiography.

Keywords: bifurcation angle, coronary CT angiography, calcified plaques, diagnostic value.

INTRODUCTION

In recent years, the role of wall shear stress has attracted much interest as a complementary explanation for plaque formation in coronary artery disease (CAD) [1-3]. The influence of blood flow in the development of atherosclerosis is based on the observation that plaques are distributed near side branches or arterial stenosis, where the flow is non-uniform, and at the lesser curvature of bends where blood flow speeds are relatively low [4, 5]. Coronary plaques appear specifically in the left coronary artery near the bifurcation angle formed by two main coronary branches where the flow is disturbed and endothelial shear stress is low [6-8].

Altered hemodynamic parameters at the bifurcation region are closely associated with the development of atherosclerosis [9, 10]. Increased bifurcation angle decreases wall shear stress, which leads to plaque proliferation [11-13]. Studies using coronary CT angiography (CCTA) or intravascular ultrasound (IVUS) have demonstrated that the wide bifurcation angle is associated with increased prevalence of CAD or the presence of high-risk plaques [13-17]. Although invasive coronary angiography (ICA) is widely used as the reference technique for confirmation of coronary stenosis, assessment of bifurcation angle by ICA could be limited due to potential foreshortening and out-of-plane magnification [18, 19]. To the best of our knowledge, there is no report on comparison of coronary bifurcation angle and lumen measurements between CCTA and ICA in patients with CAD. Thus, the purpose of this study is to investigate the diagnostic value of CCTA in coronary plaques by comparing bifurcation angle and coronary lumen measurements with ICA as the reference method. This study only focuses on the assessment of calcified plaques as it is well-known that

CCTA has low specificity and low positive predictive value in the diagnosis of calcified plaques [20-23]. Therefore, we hypothesized that the approach of measuring bifurcation angle with CCTA is more accurate than coronary lumen assessment in the diagnostic evaluation of calcified plaques.

MATERIALS AND METHODS

Study population

All patients who were referred for the assessment of CAD between March and August 2014 with CCTA and ICA examinations performed within a 4-week interval were retrospectively reviewed. Only those patients with calcified plaques (detected by CCTA) in at least one left coronary artery were included in the study. The exclusion criteria consisted of contraindications for contrast medium, previous history of coronary stenting or coronary bypass grafting, renal dysfunction or intolerance to beta-blockers. Out of 75 consecutive patients with CCTA and ICA imaging who were screened, 53 were eligible for inclusion. Reasons for exclusion were non-calcified or mixed plaques on coronary arteries (n=15), coronary stenting (n=5), and poor CCTA image quality (n=2). The patient's characteristics are summarized in Table 1. Ethics approval from institutional review board was waived in this study as acquisition of CCTA images was part of clinical examination for the diagnosis of CAD. No informed consent was obtained from the patients, given the retrospective nature of the study.

CCTA scanning protocol

The patients were scanned with a first-generation dual-source CT (Somatom Definition, Siemens Healthcare, Forchheim, Germany), or a second-generation dual-source CT (Somatom Definition Flash, Siemens Healthcare, Forchheim, Germany), or a first-generation 320-slice CT (Toshiba Aquilion ONE, Toshiba, Otawara, Japan). The CCTA scanning parameters were (i) for the first-generation dual-source CT scanner: 2 x 32 x 0.6 mm detector collimation, gantry rotation of 0.33 s, with a tube voltage of 100-120 kV depending on body mass index (BMI) and tube current ranging from 345 to 420 mAs with retrospective ECG-gating, (ii) for the second-generation dual-source CT scanner: 2 x 64 x 0.6 mm detector collimation, gantry rotation of 0.28 s, with a tube voltage of 100-120 kV depending on BMI and tube current ranging from 330 to 450 mAs with retrospective ECG-gating, and (iii) for the first-generation 320-slice CT scanner: 320 x 0.5 mm detector collimation, gantry rotation of 0.35 s, with a tube voltage of 100-120 kV depending on BMI and automatic tube current modulation with prospective ECG-gating. Beta-blockers were administered in patients with heart rate more than 65 bpm (beats per minute) for 320-slice CT scanning and in patients with heart rate more than 80 bpm for the first and second-generation dual-source CT scanning.

A bolus of non-ionic contrast medium Iopromide at 370 mg/mL (Iopromide 370, Bayer Schering Pharma) which varied between 50 and 75 mL was injected intravenously (flow rate, 4-5.5 ml/s, depending on the kV used in the scanning protocol), followed by 30 mL saline chaser. A bolus tracking technique was used to synchronize the arrival of contrast medium in the coronary arteries for initiation of the scan with CT attenuation of 120 Hounsfield unit (HU) as the triggering threshold. ECG tube current modulation was used with full tube current from 30% to 75% of the R-R interval. The pitch for the retrospectively ECG-gated scan varied from 0.2-0.4, depending on the heart rate for the first and second-generation dual-source scanners. Images were reconstructed with a slice thickness of 0.6-0.75 mm and a reconstruction interval of 0.5-0.6 mm for the first and second-generation dual-source CT, 0.5 mm and interval of 0.25 mm for 320-slice CT, respectively.

CCTA image analysis

All datasets from CCTA scans were transferred to a separate workstation equipped with Analyze V 11.0 software (AnalyzeDirect, Inc., Lexana, KS, USA) for image post-processing and analysis. Post-processing and analysis was done by two experienced assessors (with 7 and more years of experience in cardiac CT imaging), who were blinded to the results of the ICA analysis. The minimal lumen diameter (MLD) of the two main coronary arteries (left anterior descending (LAD) and left circumflex (LCx)) was measured on multiplanar/curved planar reformatted images in the views showing the highest degree of stenosis caused by calcified plaques. Right coronary artery was not assessed as this study focused on the left coronary bifurcation angle. The interval of MLD measurements in CCTA and ICA was 2 weeks. Three consecutive measurements of the MLD at each coronary lesion were obtained, and the mean value was used to avoid intra-observer disagreement. Assessors performed the measurements independently with good inter-observer agreement of 85% and intra-observer agreement of 86%.

The percentage of coronary lumen stenosis was calculated using the following formula:

$$\% \text{ coronary stenosis} = (RD-MLD)/RD \quad (1)$$

RD refers to the reference vessel diameter of normal coronary artery. The degree of coronary lumen stenosis was considered significant when the percentage of reduction was >50%. When there were multiple calcified plaques present in the coronary arteries, measurements were performed at the most severely calcified lesions.

Invasive coronary angiography

The ICA was performed by femoral or radial approach. The MLD was measured at the most severe narrowing of two main coronary arteries (LAD and LCx) by a radiologist with 15 and more years of experience in cardiac imaging. Similarly, three consecutive measurements of the MLD within the same lesion were obtained, and the mean value was considered as final.

Measurement of bifurcation angle

Bifurcation angle was measured only during diastolic phase for both CCTA and ICA, as the maximum angulation can be achieved only during diastolic phase. Three dimensional (3D) volume rendering (VR) CCTA images were reconstructed and the VR views with clear visualization of the angulation in the left coronary artery were used to determine the bifurcation angle between LAD and LCx (Fig. 1). Measurements were performed by two assessors (with 7 and more years of experience in cardiac CT imaging), who were blinded to the results of ICA. Figure 2 shows the bifurcation angle measurement in ICA. Measurements were performed by the same assessors 2 weeks later after CCTA data analysis to avoid prior knowledge of the previous measurements on CCTA images. Similar to the approach used in measurements of MLD, three consecutive measurements of the bifurcation angle were obtained and the mean value was considered as final. Assessors reported the presence of coronary plaques and coronary stenosis with regard to the corresponding bifurcation angle, with good inter-observer agreement of 91% and intra-observer agreement of 95%.

Statistical analysis

Statistical analyses were performed using SPSS 21.0 (SPSS Inc, Chicago., IL, USA). Continuous variables were expressed as mean ± standard deviation, while categorical variables were presented as percentages. All variables input to t-test procedures were first examined for normality with the Kolmogorov-Smirnov test. Sensitivity, specificity, positive predictive value (PPV) and negative predictive value (NPV) for the diagnosis of coronary stenosis (>50%) based on MLD measurement using CCTA were calculated for two coronary arteries separately with ICA as the reference method. The diagnostic value of CCTA and ICA based on bifurcation angle measurement was calculated with degree of stenosis on ICA as the reference method. Receiver-operating characteristic (ROC) curve analysis was used to assess the diagnostic performance of CCTA and ICA using these measurement approaches for diagnosis of coronary stenosis. The areas under the ROC curves (AUCs) were compared between these two imaging methods. Bland-Altman plot analysis was used to estimate the mean difference in bifurcation angle measurements between CCTA and ICA. This provides a visual indication of how the measurement bias varies in the assessment of left coronary bifurcation angle between these two imaging modalities. A p value of $< .05$ was considered statistically significant.

RESULTS

Table 1 shows the distribution of calcified plaques in these two coronary arteries. ICA showed coronary stenosis greater than 50% in 25 (47%) patients, involving a total of 28 coronary arteries.

Most of calcified plaques (61%) were found to involve the LAD, with 3 patients having two-vessel disease (LAD and LCx).

The mean bifurcation angle measured with CCTA and ICA was 81.9 ± 12.3º and 81.7 ± 11.5º respectively. The mean difference of bifurcation angle measurements between CCTA and ICA was not statistically significant (0.23º ± 6.06º, p=0.19). The Bland-Altman plots show a large amount of values near the zero bias line and a very slight positive bias of 0.23º (Fig. 3).

The sensitivity, specificity, PPV and NPV and 95% confidence interval (CI) for CCTA and ICA with use of bifurcation angle for diagnosis of CAD at LAD and LCx are presented in Table 2. By using 80º as a cut-off value for determining significant coronary stenosis, our results showed no significant difference between the diagnostic value of CCTA and ICA based on bifurcation angle measurement (p=0.80-0.92), although the specificity and PPV in ICA was slightly higher than that observed in CCTA as shown in Table 2. The AUCs by ROC curve analysis for CCTA and ICA bifurcation angle measurements demonstrated no significant difference, with the corresponding AUCs being 0.79 and 0.86 (Fig. 4A), in the LAD (p=0.13) and 0.70 and 0.68 (Fig. 4B) in the LCx (p=0.81), respectively.

The sensitivity, specificity, PPV and NPV and 95% CI for CCTA assessment of MLD at per-vessel level were 100% (84%, 100%), 18% (6%, 37%), 49% (33%, 64%) and 100% (48%, 100%) for LAD; 100% (54%, 100%), 50% (30%, 70%), 32% (12%, 56%), and 100% (75%, 100%) for LCx, respectively. The AUCs by ROC curve analysis showed significant differences between CCTA and ICA, with corresponding AUCs being 0.58 and 0.98 based on analysis of MLD in the LAD (p=0.007) (Fig. 5A), 0.67 and 0.97 (p=0.02) in the LCx (Fig. 5B), respectively.

Figure 6 is an example of a patient with calcified plaques in the LAD and LCx showing wide bifurcation angles measured on CCTA and ICA, with significant coronary stenosis confirmed on ICA, while Figure 7 shows another example of calcified plaque in the LCx, with measured narrow bifurcation angles on both techniques, and no significant stenosis on ICA.

DISCUSSION

In this study, we compared the diagnostic value of CCTA in the assessment of calcified plaques based on bifurcation angle measurements and coronary lumen changes with ICA as the reference method to determine the degree of stenosis. To the best of our knowledge, this study is the first head-to-head comparison study between CCTA and ICA to examine the diagnostic accuracy of using bifurcation angle as a criterion to diagnose coronary artery disease as opposed to coronary lumen assessment.

Main findings of this study can be summarized as follows: First, CCTA using bifurcation angle shows high diagnostic value which is comparable to that of ICA, indicating the reliability of using this approach for the assessment of calcified plaques. Second, CCTA based on MLD is still significantly affected by the presence of heavy calcification with low specificity and PPV. Thus, measurement of bifurcation angle could be recommended as an alternative to coronary lumen assessment when analyzing patients with high calcification to improve the specificity and PPV.

Advances in CT technology have improved the diagnostic value of CCTA, making it a widely used less-invasive imaging modality in the diagnosis of CAD, determination of adverse cardiovascular events and improvement of patient outcomes, leading to reduction of overall health care costs [24-

28]. Despite these promising results, it is well known that diagnosis of calcified coronary plaques using CCTA is affected by artifacts resulting from the high calcium scores in the coronary artery, thus compromising the specificity and PPV as well as prognostic value of major adverse cardiac events [29]. The reported specificity of CCTA ranges from 19% to 53% in patients with highly calcified plaques [20, 22, 23, 30], according to the assessment of coronary lumen stenosis. Finding in our study are consistent with these results, with very low specificity (18%) noticed in the LAD, and low PPV (32-49%) noticed in both LAD and LCx, further confirming the limited value of CCTA in the diagnosis of calcified plaques. The limitation of standard CCTA can be overcome with a newly introduced high-definition CT scanner with substantially improved in-plane spatial resolution of 0.23 mm, therefore, reducing beam hardening and blooming artifacts due to heavy calcification in coronary plaques [31]. Pontone et al compared the diagnostic value of high spatial resolution (0.23 mm) with standard spatial resolution (0.625 mm) CCTA in 184 patients at high risk for CAD by using ICA as the reference method [32]. In a segment-based analysis, the specificity and PPV were 98% and 91% for high resolution CCTA, which is significantly higher than the 95% and 80% for standard CCTA. No differences were found in the assessment of non-calcified or mixed plaques between the two groups, however, the overall agreement between CCTA and ICA was significantly improved in the analysis of calcified plaques for high resolution CCTA when compared to the standard CCTA (83%, 91%, 85% and 73% vs 53%, 58%, 51% and 49%, corresponding to all, small, moderate and large calcified plaques, respectively).

In contrast, previous studies have shown that using bifurcation angle to diagnose CAD improves the diagnostic performance with wide angulation associated with diseased coronary arteries and high-risk plaques [14, 17, 33, 34]. High-risk plaques were found to be associated with higher bifurcation angles when compared to the normal coronary arteries, indicating the correlation between wide bifurcation angle and plaque formation and development of high-risk plaques. A strong correlation between low shear stress and endothelial dysfunction and atherosclerotic lesions in the arterial bifurcations or in areas of abrupt curvatures has been well established [5, 35, 36]. Shear stress is well known to play an important role in both early plaque formation and progression [5, 37]. Furthermore, bifurcation angle variation also plays a vital role in atherosclerosis development: the larger the bifurcation angle, the greater the turbulence and the greater the hemodynamic impact in the arterial regions [5, 38]. Results from our study are in accordance with previous observation, as the specificity and PPV is close to 80% for CCTA and more than 80% for ICA, showing the reliability of using the bifurcation angle approach in the analysis of calcified plaques mainly because of a reduced overestimation of coronary artery stenoses. Therefore, measurement of bifurcation angle could be incorporated into the routine diagnostic assessment of coronary artery disease, especially in those with calcified plaques.

The importance of bifurcation angle has been well recognized in the area of bifurcation intervention, since bifurcation angulations can impact both peri-procedural and long-term outcomes of percutaneous coronary intervention (PCI) [39-41]. However, the exact relationship between bifurcation angle and coronary artery disease has not been fully elucidated. Rodriguez-Granillo GA et al. measured bifurcation angles using CCTA in 50 patients and their results showed that the median bifurcation angle was 88.5º, with close association between wide angles and LAD or LCx disease [42]. The natural distribution of bifurcation angles by CCTA were between 72 ± 22º and 80

± 27º, according to previous studies [15, 16]. This supports our criterion of using 80º as cut off to determine the coronary artery disease. However, these previous reports only compared the bifurcation angles between normal and diseased coronary arteries, while in this study we extended the application of using bifurcation angle to address a challenging area in CCTA, which is the diagnostic value of CCTA in patients with calcified plaques. With high prevalence of diseased coronary arteries in the selected patients, this study shows high diagnostic accuracy of using bifurcation angle for diagnosis of coronary artery disease by CCTA with excellent correlation to ICA, although further research based on a large sample size is needed to support our findings.

Invasive coronary angiography is the gold standard for the identification of obstructive coronary lesions. However, it lacks the sensitivity and specificity for the early detection of the vulnerable plaque. The role of ICA is gradually diminishing as compared to other imaging modalities such as CCTA or IVUS, which are able to look beyond the lumen and characterize plaque morphology or vessel wall [43, 44]. The limited diagnostic value of CCTA for coronary lumen analysis in calcified plaques is demonstrated in this study. However, the high diagnostic performance of CCTA by measuring bifurcation angle compared to ICA indicates that CCTA can be used as an alternative to ICA when diagnosing the calcified plaques.

There are some limitations in this study. First, the study is limited by the retrospective, single-center design with a small sample size. Further studies based on a large population, preferably in a multicenter trial with an established follow-up period are needed. Second, only calcified plaques were analyzed while other types of plaques were excluded. This can be explained by the fact that calcified plaques present a major challenge to the diagnostic value of CCTA. Third, despite a direct comparison of CCTA findings with ICA in this study, no treatment outcomes such as PCI are available, thus, it is difficult to assess how the bifurcation angles impact the selection of treatment strategies. Finally, all bifurcation angles were obtained using 2D angiographic images, while 3D quantitative analysis allows for more accurate measurement of bifurcation angles, as suggested by some researchers [45, 46]. Although several 3D quantitative coronary angiography programs are available, discordant results have been reported regarding the accuracy of using this technique for bifurcation angle measurements [47-49]. Our analysis shows a very good correlation between 3D CCTA and 2D ICA measurements of bifurcation angle, although attention should be paid when performing ICA measurements due to presence of large variabilities in optimal viewing angles [50].

In conclusion, this study extends the application of using bifurcation angle by CCTA beyond the lumen assessment of coronary artery disease by showing high diagnostic value of CCTA in patients with calcified plaques. A good correlation is found between CCTA and ICA in using bifurcation angle measurement for determination of coronary artery stenosis with wide angulation associated with significant coronary stenosis. CCTA by bifurcation angle can be used as a reliable alternative to ICA when assessing the calcified plaques.

Acknowledgements

This work has been supported by research grant for Excellent Talents from Beijing city (2011D003034000030), and grant for High Levels of Health Technical Personnel in Beijing City Health System (2013-3-011). We thank Mr Gil Stevenson for his assistance in the data analysis.

Conflict of Interest

The authors declared that there is no conflict of interest in this study.

References

[1] Shaaban AM, Duerinckx AJ. Wall shear stress and early atherosclerosis: a review. AJR Am. J. Roentgenol. 174 (2000) 1657–1665.

[2] Cunningham KS, Gotlieb AI. The role of shear stress in the pathogenesis of atherosclerosis. Lab. Invest. 85 (2005) 85:9–23.

[3] Sun Z, Xu L. Computational fluid dynamics in coronary artery diseases. Comput. Med. Imaging. Graph. 38 (2014) 651-663.

[4] Davies PF, Polacek DC, Shi C, Helmke BP. The convergence of haemodynamics, genomics, and endothelial structure in studies of the focal origin of atherosclerosis. Biorheology. 39 (2002) 299–306.

[5] Chaichana T, Sun Z, Jewkes J. Computation of hemodynamics in the left coronary artery with variable angulations. J. Biomech. 44 (2011)1869-1878.

[6] Caro CG, Fitz-Gerald JM, Schroter RC. Arterial wall shear and distribution of early atheroma in man. Nature. 223 (1969)1159–1160.

[7] Friedman MH, Hutchins GM, Bargeron CB, Deters OJ, Mark FF. Correlation between intimal thickness and fluid shear in human arteries. Atherosclerosis. 39 (1981) 425–436.

[8] Wentzel JJ, Chatzizisis YS, Gijsen FJH, Giannoglou GD, Feldman CL, Stone PH. Endothelial shear stress in the evolution of coronary atherosclerotic plaque and vascular remodelling: current understanding and remaining questions. Cardiovasc. Res. 96 (2012) 234-243.

[9] Markl M, Wegent F, Zech T, et al. In vivo wall shear stress distribution in the carotid artery: Effect of bifurcation geometry, internal carotid artery stenosis, and recanalization therapy. Circ. Cardiovasc. Imaging. 3 (2010) 647–655.

[10] Arjmandi Tash O, Razavi SE. Numerical investigation of pulsatile blood flow in a bifurcation model with a non-planar branch: The effect of different bifurcation angles and non-planar branch. Bioimpacts. 2 (2012) 195–205.

[11] Kimura BJ, Russo RJ, Bhargava V, et al. Atheroma morphology and distribution in proximal left anterior descending coronary artery: In vivo observations. J. Am. Coll. Cardiol. 27 (1996) 825–831.

[12] Kaazempur-Mofrad MR, Isasi AG, Younis HF, et al. Characterization of the atherosclerotic carotid bifurcation using MRI, finite element modeling, and histology. Ann. Biomed. Eng. 32 (2004) 932–946.

[13] Rodriguez-Granillo GA, Garcia-Garcia HM, Wentzel J, et al. Plaque composition and its relationship with acknowledged shear stress patterns in coronary arteries. J. Am. Coll. Cardiol. 47 (2006) 884–885.

[14] Sun Z, Cao Y. Multislice CT angiography assessment of left coronary artery: Correlation between bifurcation angle and dimensions and development of coronary artery disease. Eur. Radiol. 79 (2011) e90–e95.

[15] Kawasaki T, Koga H, Serikawa T, et al. The bifurcation study using 64 multislice computed tomography. Catheter. Cardiovasc. Interv. 73 (2009) 653-658.

[16] Pflederer T, Ludwig J, Ropers D, Daniel WG, Achenbach S. Measurement of coronary artery bifurcation angles by multidetector computed tomography. Invest. Radiol. 41 (2006) 793–798.

[17] Papadopoulou SL, Brugaletta S, Garcia-Garcia HM, et al. Assessment of atherosclerotic plaques at coronary bifurcations with multidetector computed tomography angiography and intravascular ultrasound-virtual histology. Eur. Heart. J. Cardiovasc. Imaging. 13 (2012) 635-642.

[18] Green NE, Chen SY, Messenger JC, Groves BM, Carroll JD. Three-dimensional vascular angiography. Curr. Probl. Cardiol. 29 (2004) 104–42.

[19] Reiber JHC, Serruys PW, Kooijman CJ, et al. Assessment of short-, medium-, and long-term variations in arterial dimensions from computer-assisted quantitation of coronary cineangiograms. Circulation. 71 (1985) 280–288.

[20] Park MJ, Jung JI, Choi YS, et al. Coronary CT angiography in patients with high calcium score: evaluation of plaque characteristics and diagnostic accuracy. Int. J. Cardiovasc. Imaging. 27 (2011) 43-51.

[21] Sun Z, Ng C. High calcium scores in coronary CT angiography: effects of image post-processing on visualization and measurement of coronary lumen diameter. J. Med. Imaging. Health. Inf. 5 (2015) 110-116.

[22] Chen CC, Chen CC, Hsieh IC, et al. The effect of calcium score on the diagnostic accuracy of coronary computed tomography angiography. Int. J. Cardiovasc. Imaging. Suppl 1 (2011) 37-42.

[23] Palumbo A, Maffei E, Martini C, et al. Coronary calcium score as gatekeeper for 64-slice computed tomography coronary angiography in patients with chest pain: per-segment and per-patient analysis. Eur. Radiol. 19 (2009) 2127-35.

[24] Sara L, Rochitte CE, Lemos PA, et al. Accuracy of multidetector computed tomography for detection of coronary artery stenosis in acute coronary syndrome compared with stable coronary disease: A CORE64 multicenter trial subsidy. Int. J. Cardiol. 177 (2014) 385-391.

[25] Funabashi N, Uehara M, Takaoka H, et al. A two center 320 slice CT study for evaluating coronary arteries in subjects with chronic atrial fibrillation: A comparison of prospective and retrospective ECG-gating acquisition. Int. J. Cardiol. 177 (2014) 374-379.

[26] Rajani R, Webb J, Marciniak A, Preston R. Comparative efficacy testing-fractional flow reserve by coronary computed tomography for the evaluation of patients with stable chest pain. Int. J. Cardiol. 183 (2015)173-177.

[27] Habib PJ, Green J, Butterfield RC, et al. Association of cardiac events with coronary artery disease detected by 64-slice or greater coronary CT angiography: A systematic review and meta-analysis. Int. J. Cardiol. 169 (2013) 112-120.

[28] Takaoka H, Funabashi N, Fujumoto Y, Kobayashi Y. Detection of significant stenosis in the left anterior descending artery by 'virtual myocardial perfusion' bolus tracking, 320 sliced computed tomography. Int. J. Cardiol. 177 (2014) 1001-1007.

[29] Uehara M, Funabashi N, Takaoka H, Fujimoto Y, Kobayashi Y. False-positive findings in 320-slice cardiac CT for detection of severe coronary stenosis in comparison with invasive coronary angiography indicate poor prognosis for occurrence of MACE. Int. J. Cardiol. 172 (2014) 235-237.

[30] Meng L, Cui L, Cheng Y, et al. Effect of heart rate and coronary calcification on the diagnostic accuracy of the dual-source CT coronary angiography in patients with suspected coronary artery disease. Korean. J. Radiol. 10 (2009) 347-54.

[31] Machida H, Tanaka I, Fukui R, et al. Current and novel imaging techniques in coronary CT. Radiographics. 35 (2015) 991-1010.

[32] Pontone G, Bertella E, Mushtaq S, et al. Coronary artery disease: diagnostic accuracy of CT coronary angiography-A comparison of high and standard spatial resolution scanning. Radiology. 271 (2014) 688-694.

[33] Sun Z. Coronary CT angiography in coronary artery disease: correlation between virtual intravascular endoscopic appearances and left bifurcation angulation and coronary plaques. Biomed. Res. Int. 2013 (2013) 732059.

[34] Xu L, Sun Z. Coronary CT angiography evaluation of calcified coronary plaques by measurement of left coronary bifurcation angle. Int. J. Cardiol. 182 (2015) 229-231.

[35] Nakazawa G, Yazdani SK, Finn AV, Vorpahl M, Kolodgie FD, Virmani R. Pathological findings at bifurcation lesions: The impact of flow distribution on atherosclerosis and arterial healing after stent implantation. J. Am. Coll. Cardiol. 55 (2010) 1679-1687.

[36] Katritsis D, Kaiktsis L, Chaniotis A, Pantos J, Efstathopoulos EP, Marmarelis V. Wall shear stress: theoretical considerations and methods of measurement. Prog. Cardiovasc. Dis. 49 (2007) 307-327.

[37] Stone PH, Saito S, Takahashi S, et al. Prediction of progression of coronary artery disease and clinical outcomes using vascular profiling of endothelial shear stress and arterial plaque characteristics: the PREDICTION study. Circulation. 126 (2012) 172-181.

[38] Perktold K, Peter RO, Resch M, Langs G. Pulsatile non-Newtonian blood flow in three-dimensional carotid bifurcation models: a numerical study of flow phenomena under different bifurcation angles. J. Biomed. Eng. 13 (1991) 507-515.

[39] Kralev S, Poerner TC, Basorth D, et al. Side branch occlusion after coronary stent implantation in patients presenting with ST elevation myocardial infarction: Clinical impact and angiographic predictors. Am. Heart. J. 151 (2006) 153–157.

[40] Vassilev D, Alexandrov A, Le D, et al. Importance of bifurcation angle in bifurcation stenting. Chin. Med. J. (Engl). 125 (2012) 4122–4125.

[41] Zhang D, Xu B, Yin D, et al. How bifurcation angle impacts the fate of side branch after main vessel stenting: A retrospective analysis of 1,200 consecutive bifurcation lesions in a single center. Catheter. Cardiovasc. Interv. 85 Suppl 1 (2015) 706-715.

[42] Rodriguez-Granillo GA, Rosales MA, Degrossi E, Durbano I, Rodriguez AE. Multislice CT coronary angiography for the detection of burden, morphology and distribution of atherosclerotic plaques in the left main bifurcation. Int. J. Cardiovasc. Imaging. 23 (2007) 389-392.

[43] Chan KH, Ng MKC. Is there a role for coronary angiography in the early detection of the vulnerable plaque? Int. J. Cardiol.164 (2013) 262-266.

[44] Colombo A, Panoulas VF. Diagnostic coronary angiography is getting old. JACC. Cardiovasc. Imaging. 8 (2015) 11-13.

[45] Ng VG, Lansky AJ. Novel QCA methodologies and angiographic scores. Int. J. Cardiovasc. Imaging. 27 (2011) 157-165.

[46] Girasis C, Farooq V, Diletti R, et al. Impact of 3-dimensional bifurcation angle on 5-year outcome of patients after percutaneous coronary intervention for left main coronary artery disease: A substudy of the SYNTAX trial (Synergy Between Percutaneous Coronary Intervention With Taxus and Cardiac Surgery). J. Am. Coll. Cardiol. Interv. 61 (2013) 1250-1260.

[47] Ramcharitar S, Daeman J, Patterson M et al. First direct in vivo comparison of two commercially available three-dimensional quantitative coronary angiography systems. Catheter. Cardiovasc. Interv. 71 (2008) 44–50.

[48] Dvir D, Marom H, Guetta V, Kornowski R. Three dimensional coronary reconstruction from routine single plane coronary angiograms: in vivo quantitative validation. Int. J. Cardiovasc. Intervent. 7 (2005) 141–145.

[49] Tu S, Koning G, Jukema W, Reiber JH. Assessment of obstruction length and optimal viewing angle from biplane X-ray angiograms. Int. J. Cardiovasc. Imaging. 26 (2010) 5–17.

[50] Tu S, Jing J, Holm NR, et al. In vivo assessment of bifurcation optimal viewing angles and bifurcation angles by three-dimensional (3D) quantitative coronary angiography. Int. J. Cardiovasc. Imaging. 28 (2012) 1617-1625.

Figures and figure legends

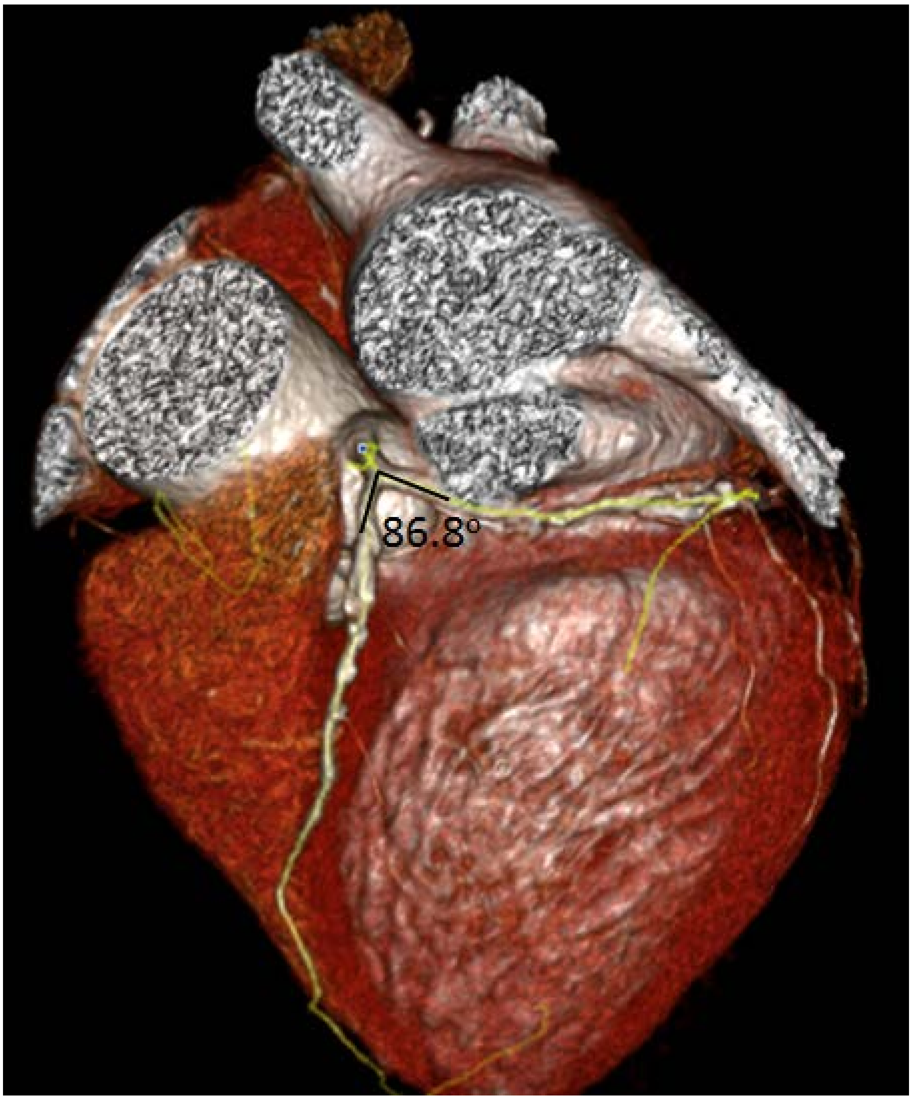

Figure 1. Bifurcation angle between left anterior descending (LAD) and left circumflex (LCx) is measured 86.8° on a 3D volume rendering image in a 54-year-old man with multiple calcified plaques at both coronary arteries.

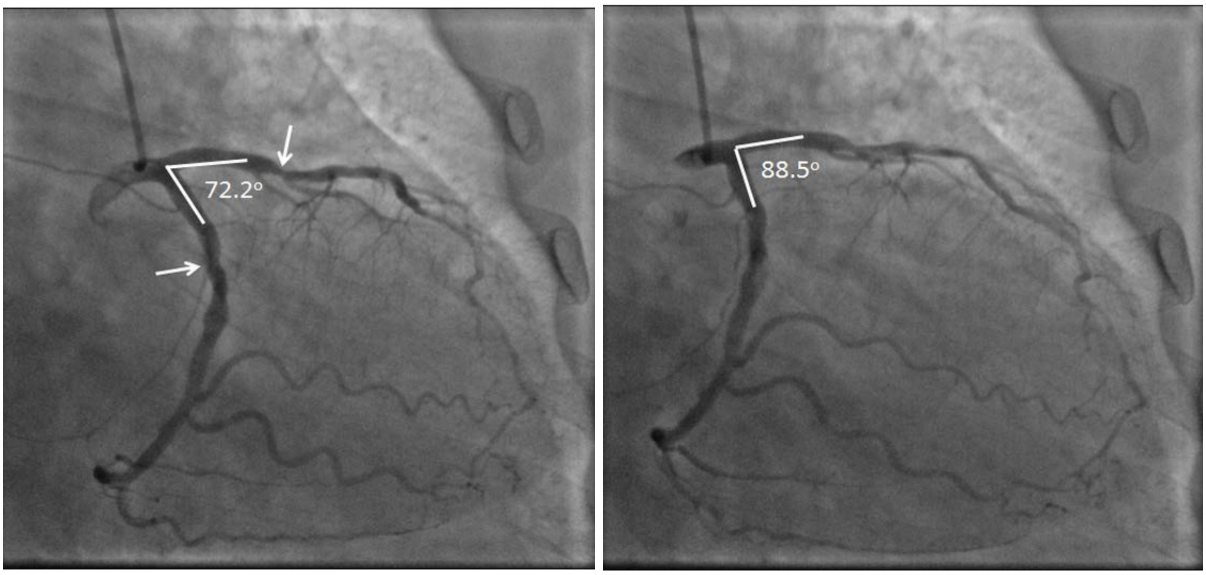

Figure 2. Same patient as in Figure 1. A: Bifurcation angle between LAD and LCx is measured 72.2º during the systolic phase on invasive coronary angiography (ICA) image. B: The bifurcation angle is measured 88.5º during the diastolic phase on ICA image, indicating the significant difference of measurements between these two cardiac phases. Arrows refer to the stenosis on both coronary arteries.

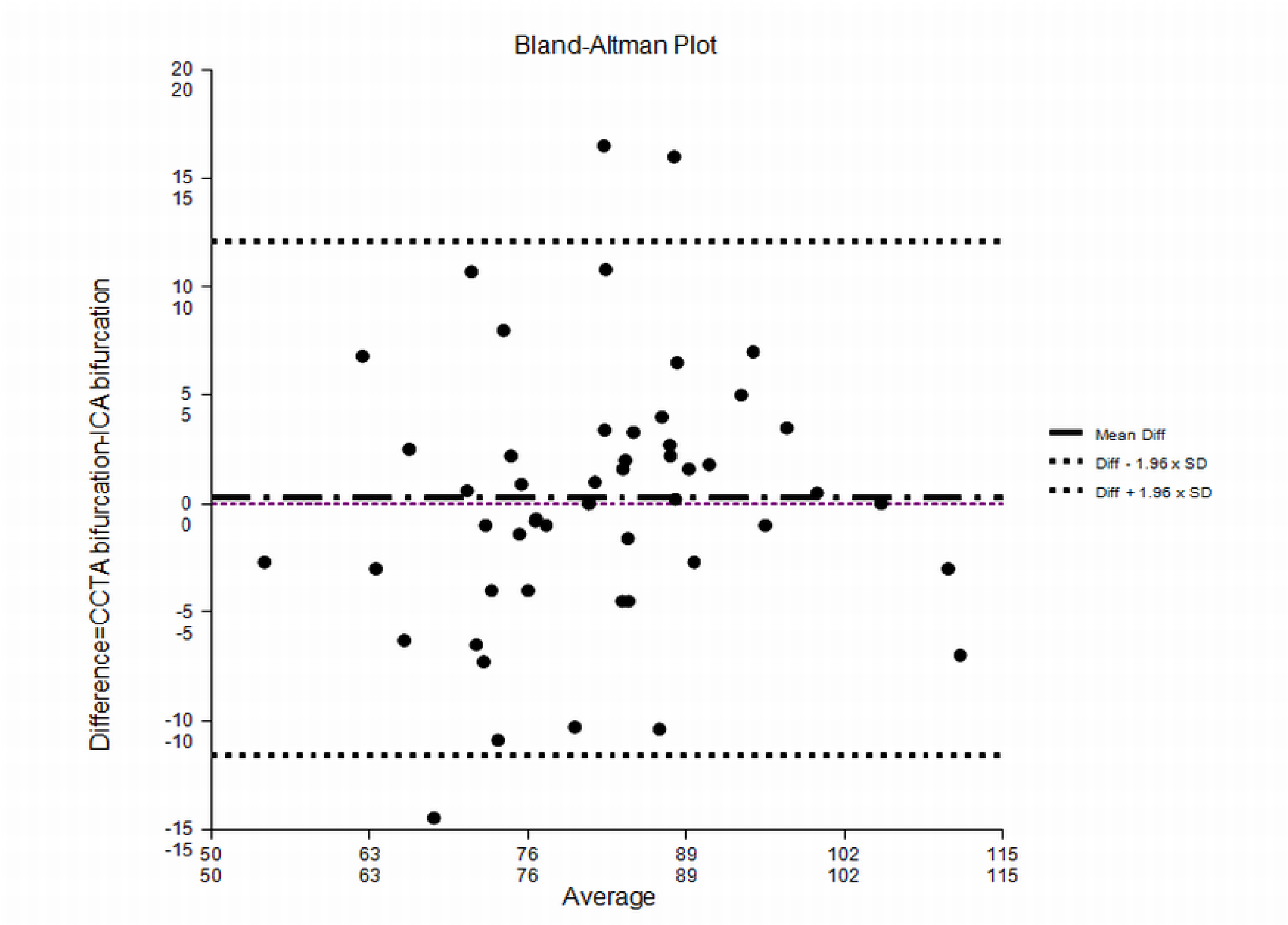

Figure 3. Bland-Altman plots of coronary CT angiography (CCTA) vs invasive coronary angiography (ICA) bias, showing line of mean bias (0.23º) and 95% tolerance limits above zero bias.

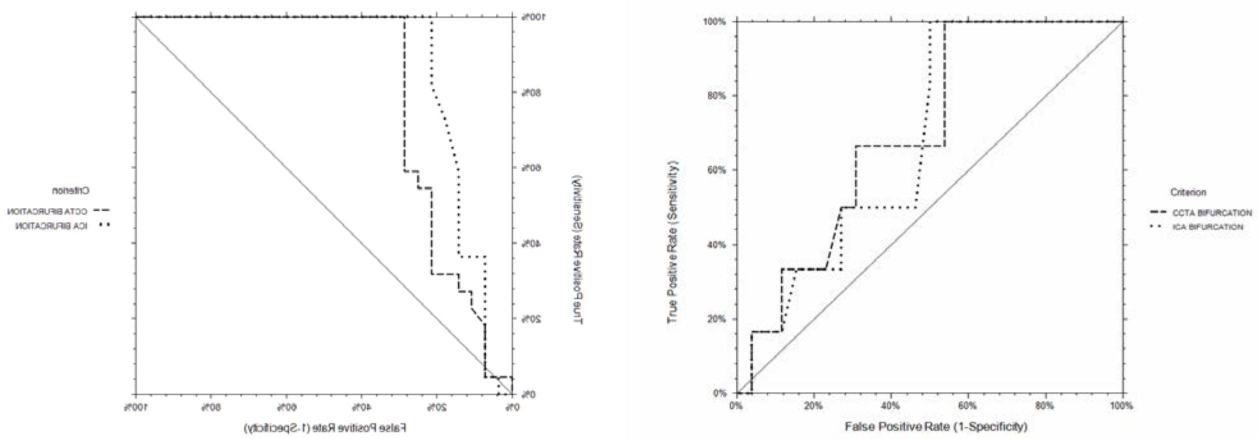

Figure 4. AUCs by receiver-operating characteristic curve analysis demonstrate the diagnostic performance of CCTA by bifurcation angle in the diagnosis of coronary stenosis when compared to

ICA by bifurcation at LAD and LCx (A, B). There is no significant difference between CCTA and ICA by bifurcation angle measurements at these two coronary arteries.

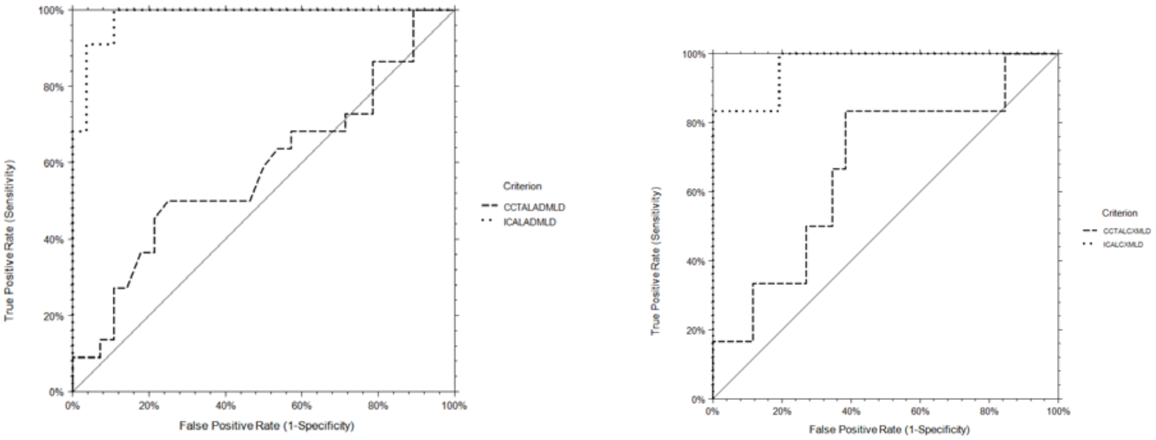

Figure 5. AUCs by receiver-operating characteristic curve analysis demonstrate the diagnostic performance of CCTA by minimal lumen diameter analysis in the detection of coronary stenosis when compared to ICA at LAD and LCx (A, B). Significant difference is found between CCTA and ICA with CCTA significantly overestimating the coronary lumen stenosis due to calcified plaques.

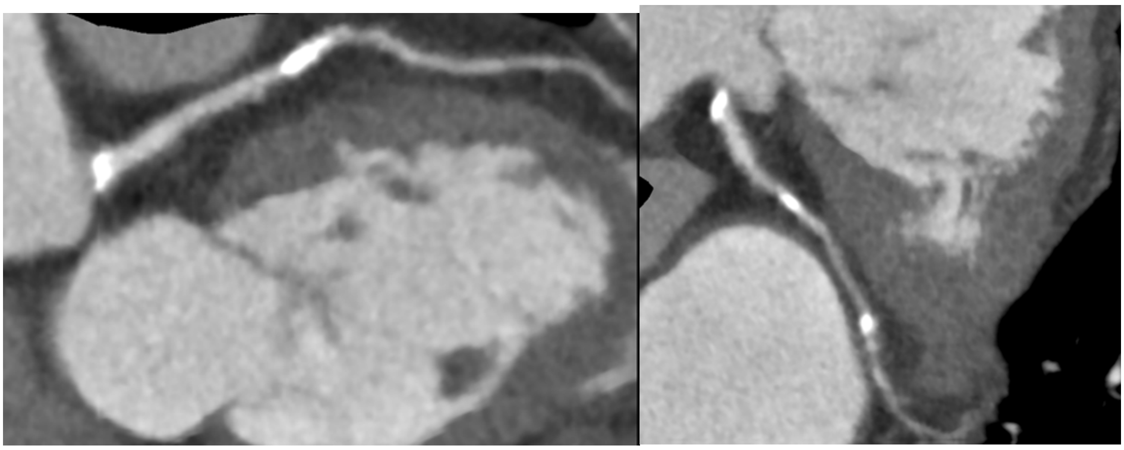

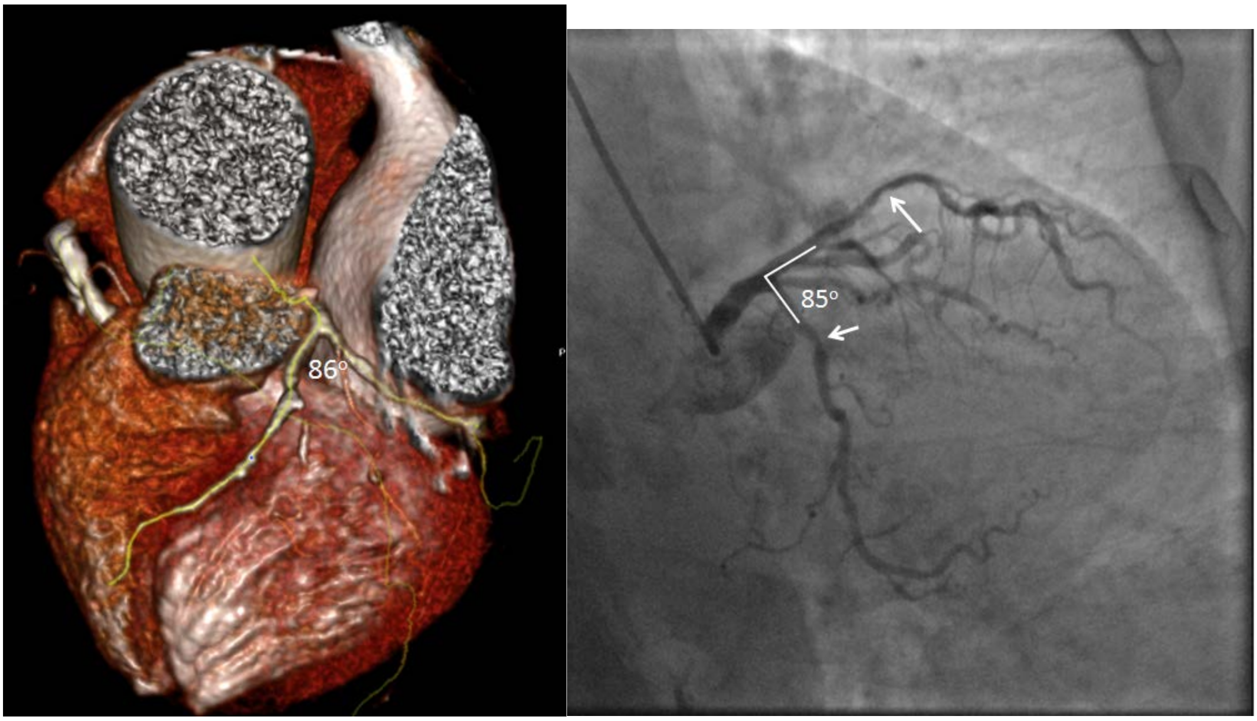

Figure 6. A and B: Curved planar reformatted CCTA images show multiple calcified plaques at the proximal segment of LAD and LCx in a 57-year-old man. C: 3D volume rendering CT demonstrates wide angulation with bifurcation angle measured 86º. D: Bifurcation angle is measured 85º on ICA image, with significant stenosis at the proximal segment of LAD (long arrow), but no significant stenosis in the LCx (short arrow).

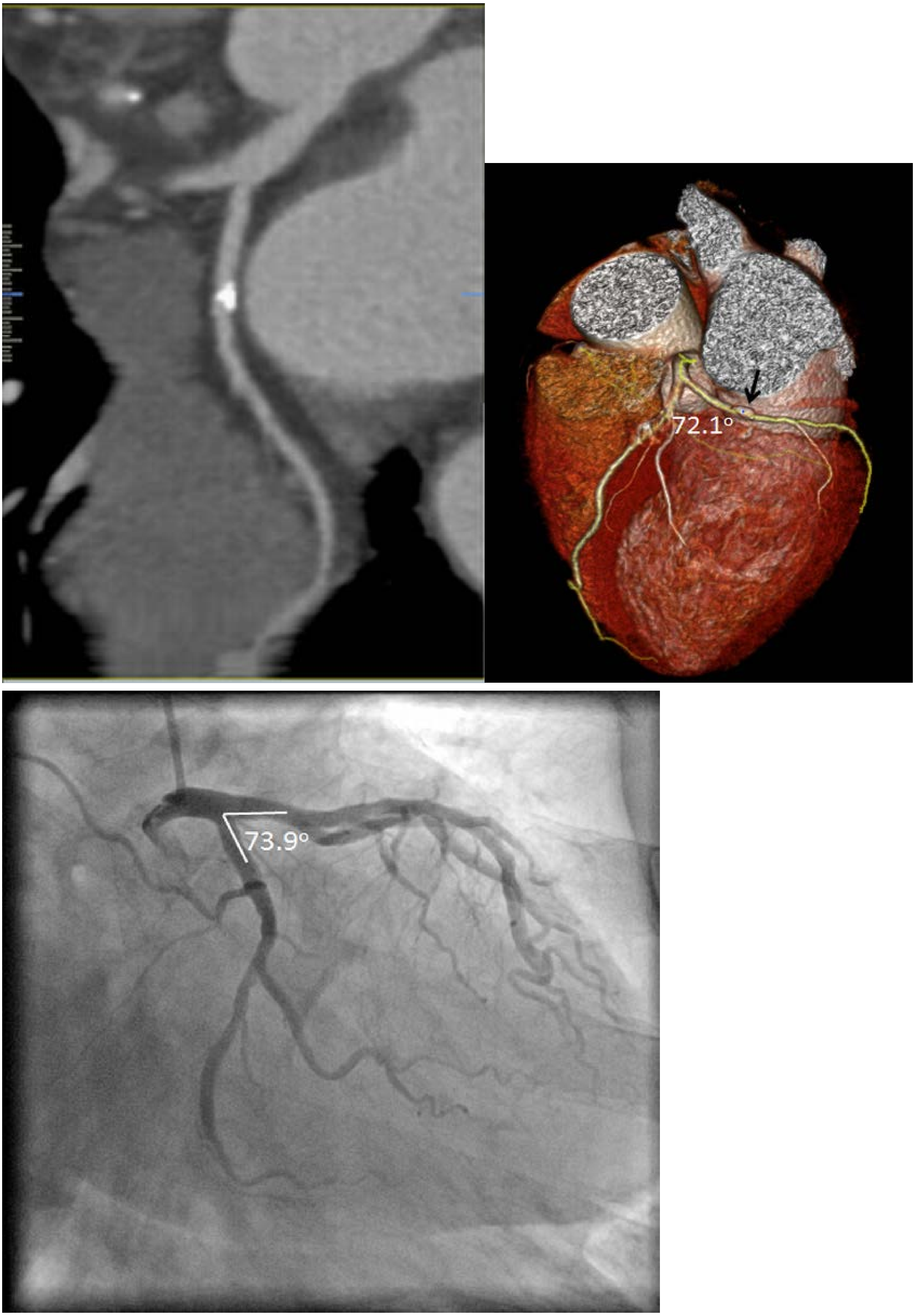
72.1°
73.9°

Figure 7. A: Curved planar reformatted CCTA image shows a calcified plaque at the proximal segment of LCx in a 69-year-old man. B and C: Bifurcation angle is measured 72.1º and 73.9 º on 3D volume rendering and ICA images, respectively, with no significant stenosis on LCx. Arrow refers to the plaque at LCx.